# Automating the high-throughput screening of protein-based optical indicators and actuators

Jihwan Lee[1], Beatriz Campillo[1], Shaminta Hamidian[1], Zhuohe Liu[3], Matthew Shorey[1], François St-Pierre[1,2,3,4,*]

1) Department of Neuroscience, Baylor College of Medicine, Houston, TX 77030, USA.
2) Systems, Synthetic, and Physical Biology Program, Rice University, Houston, TX 77005, USA.
3) Department of Electrical and Computer Engineering, Rice University, Houston, TX 77005, USA.
4) Department of Biochemistry and Molecular Biology, Baylor College of Medicine, Houston, TX, USA

* Corresponding author. E-mail: stpierre@bcm.edu

***Abstract***

Over the last 25 years, protein engineers have developed an impressive collection of optical tools to interface with biological systems: indicators to eavesdrop on cellular activity and actuators to poke and prod native processes. To reach the performance level required for their downstream applications, protein-based tools are usually sculpted by iterative rounds of mutagenesis. In each round, libraries of variants are made and evaluated, and the most promising hits are then retrieved, sequenced, and further characterized. Early efforts to engineer protein-based optical tools were largely manual, suffering from low throughput, human errors, and tedium. Here, we describe approaches to automating the screening of libraries generated as colonies on agar, multiwell plates, and pooled populations of single-cell variants. We also briefly discuss emerging approaches for screening, including cell-free systems and machine learning.

***Main text***

To unravel the enormous complexity of biological systems, life scientists rely on complementary devices: indicators to report on cellular activity (**Fig. 1A**) and actuators to modulate or perturb native processes (**Fig. 1B**). Optical indicators and actuators are particularly coveted because these devices enable visualization and modulation of cellular activity with high spatiotemporal resolution [1]. Optical devices can be based on proteins, organic dyes, RNA aptamer-dye or protein-dye pairs, and other nanomaterials [2–6]. Here, we focus on protein-based optical devices (PODs) because they are widely used and can be selectively expressed in distinct cell types to elucidate their respective functions *in vivo* [7,8].

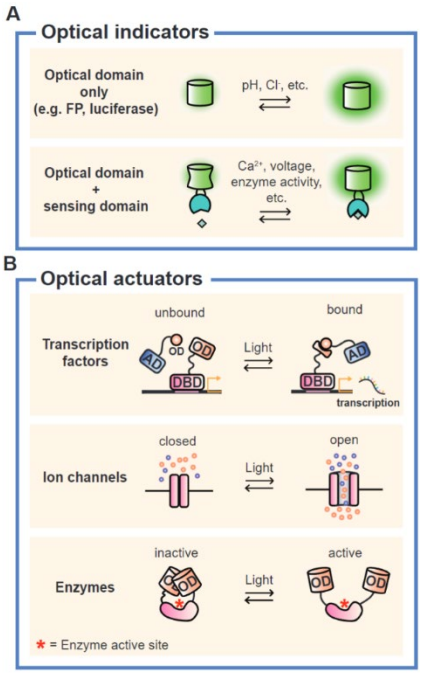


**Figure 1. Schematic illustration of various types of optical indicators and actuators.** OD: Optical domain. DBD: DNA binding domain. AD: Activating domain.

Development spanning more than two decades has produced an impressive catalog of protein-based optical indicators that report a wide range of modalities, including calcium, chloride, pH, ATP, metabolites, cAMP, voltage, neurotransmitters, and enzymatic activity [9–12]. We also consider fluorescent proteins (FPs) as indicators since they can be used to report on various aspects of cellular activity, including protein localization, gene expression, and cell cycle progression [13]. There has also been explosive growth in the number of optical actuators, including light-controllable channels, enzymes, binding domains, and transcription factors [14–17]. While this Perspective focuses on approaches deployed for automating POD development, many of the strategies discussed also apply to engineering nucleic acids and other classes of proteins. The approaches described in this article are summarized in Table 1.

Despite impressive advances with *de novo* protein design [18], PODs are usually engineered by repurposing naturally existing protein domains and optimizing their performance by screening. A common iterative screening approach is directed evolution [19,20]. In this method, molecules like PODs are mutagenized to create libraries of genetically diverse variants. These variants are then assayed to identify mutants with improved characteristics. Top-performing variants become new starting templates for the next round of screening. Generating libraries with diverse variants is critical for productive POD screening. Here, we do not discuss library generation but refer the readers to other reviews [21,22].

| | Manual colony screening | Automated colony screening | Automated screening with multiwell plates | Automated pooled screening using flow cytometry | Automated microscopy-based pooled screening |
|---|---|---|---|---|---|
| **Cell types used for screening**[a] | Bacteria<br>Yeast | Bacteria<br>Yeast | Bacteria<br>Yeast<br>Mammalian cells | Bacteria<br>Yeast<br>Mammalian cells | Bacteria<br>Yeast<br>Mammalian cells |
| **Screening throughput (variants per day)** | $10^4$ - $10^5$ | $10^4$ - $10^5$ | $10^2$ – $10^3$ | $10^6$ - $10^8$ | $10^4$ - $10^5$ |
| **Typical number of plates/tubes per day** | 10s - 100s of agar plates | 10s - 100s of agar plates | 10s of multiwell plates | One tube | One 35-mm dish or one well of a 24-well plate |
| **Operation cost per variant**[b] | Low | Low | High (with mammalian cells) | Low | Low |
| **Ability to evaluate spatial properties in individual cells** | No | No | Yes | Yes, when using imaging FACS | Yes |
| **Ability to evaluate temporal properties** | No/minimal | No/minimal | Yes | No/minimal | Yes |
| **Example Usage**[c] | **FPs**<br>Clover GFP & mRuby RFP [24]<br>mGreenLantern [29]<br><br>**Indicators**<br>***Calcium***<br>NIR-GECO1 [31]<br>***Glutamate***<br>iGluSnFR3 [32] | **FPs**<br>mCarmine [33]<br>Rosmarinus [39]<br><br>**Indicators**<br>***Glutamate***<br>iGluSnFR3 [32] | **FPs**<br>miRFP2 [87]<br><br>**Indicators**<br>***Calcium***<br>GCaMP3 [88]<br>GCaMP6 [50]<br>NIR-GECO1 [31]<br>***Voltage***<br>JEDI-2P [38]<br><br>**Actuators**<br>Light-inducible dimers[90]<br>ChannelrhodopsinChromeQ [89]<br>Light-gated calcium channel [91] | **FPs**<br>EGFP [55]<br>miRFP2 [87]<br>mPlum & mRaspberry [53]<br><br>**Indicators**<br>***Voltage***<br>Archon1 & Archon2 [66]<br>QuasAr6a & QuasAr6b [69] | **FPs**<br>mGold [68]<br><br>**Indicators**<br>***Voltage***<br>Archon1 & Archon2 [66]<br>QuasAr6a & QuasAr6b [69] |

**Table 1. Comparing different manual and automated POD screening methods.**

[a] Some screening methods (e.g., multi-well and microscope-based pooled screening) do not require cells and can be achieved with purified proteins or cell-free extracts.

[b] Excluding equipment costs (i.e., molecular biology tools, microscope systems, cell sorters)

[c] Some PODs are listed in multiple columns because they were screened using multiple methods

Optimization of many PODs has been achieved by manual library screening. For example, most engineered fluorescent proteins (FPs) have been identified by visual inspection of stacks of Petri dishes harboring bacterial colonies expressing different FP variants (**Fig. 2A**). If the fluorescence of a colony expressing a mutated construct appeared higher than the fluorescence of colonies expressing the library template, the mutant colony was manually

picked using a pipette tip or toothpick and considered for further evaluation [23–25]. As another example, light-gated channelrhodopsins used for optogenetics — i.e., the optical control of neural activity with protein-based actuators [26]— are routinely screened by manually measuring light-driven currents in individual cells using patch-clamp electrophysiology [27,28].

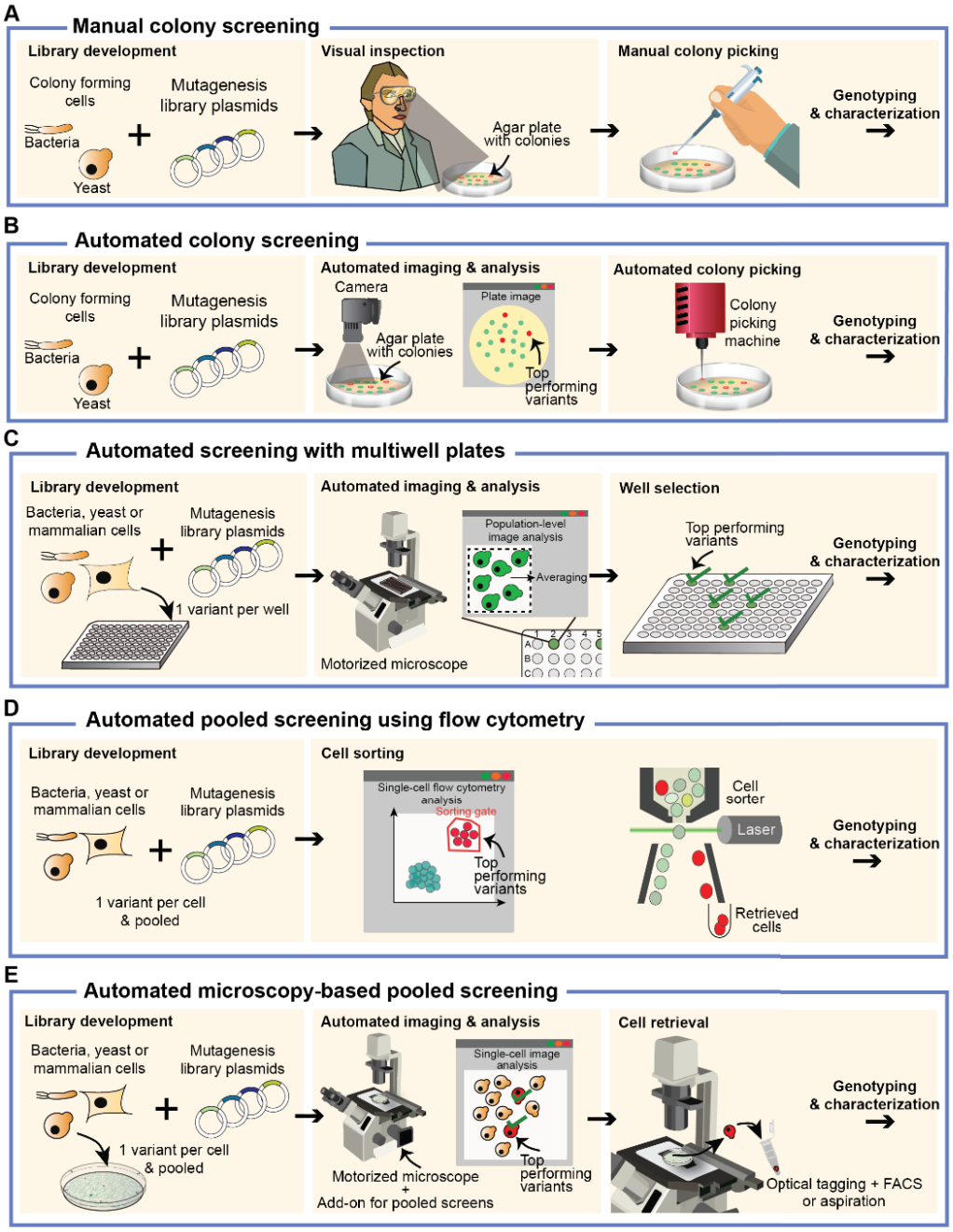


**Figure 2. Manual and automated workflows for screening Protein-based Optical Devices (PODs).**

Manual screening continues to be used [29–32] because it is simpler and often requires less expensive equipment than automated screening, in which most steps are outsourced to computers and motorized instruments. However, automation is desirable to increase screening throughput, as extensive improvements in performance are more likely achieved when screening a larger number of variants, avoiding repetitive tasks, increasing measurement sensitivity and precision, and reducing day-to-day and person-to-person variability. Also, automated approaches often involve the use of cameras or other hardware that enable the detection of a wider variety of POD properties that would otherwise be difficult or impossible to quantify using manual visual inspection with the naked eye. These properties include dim signals, emission outside the visible spectrum, fluorescence lifetime, organelle localization, temporal responses, and Förster resonance energy transfer (FRET). The feasibility and cost of automation will depend on the property being screened. For example, automation can be easily implemented for screening many optical properties, such as indicator brightness. In contrast, other properties, such as channelrhodopsin conductance and rectification, can be expensive and/or challenging to evaluate without a human expert.

***Automating the screening of bacterial or yeast colonies on agar plates***

In the past decade, many exciting new automated methods have been developed to accelerate POD screening. One approach is to automate the tedious manual steps when screening bacterial or yeast colonies on agar plates (**Fig. 2B**). For example, an automated and affordable colony evaluation and picking system was developed by combining fluorescence imaging and robotic picking of bacterial colonies [33]. This system can evaluate up to 100,000 colonies in ~ 11 hours within a single screening experiment. While an experienced FP engineer can evaluate plates at a similar speed, this platform enables screening over longer durations than typical experimentalists can sustain, thereby increasing the number of colonies screened per experiment. The authors used this automated system to develop a far-red FP 4-5 times brighter than its parental protein.

Several automated procedures were developed because detecting specific POD properties was impractical or impossible with the human eye. For example, while two-photon (2P) microscopy is a method of choice for deep-tissue imaging [34,35], there are no methods to visually inspect and manually screen fluorescent bacterial colonies illuminated by a 2P laser. Because FPs' brightness and photostability evaluated under one-photon (1P) and two-photon (2P) excitations are poorly correlated [36,37], it is imperative to screen FPs and FP-based indicators directly under 2P illumination [38]. A method for enabling and automating the 2P screening of bacterial colonies expressing FP variants was developed: plates were first imaged under 1P to identify the location of the colonies; a motorized stage moved the plates to a 2P imaging station for automated brightness quantification of individual colonies (10,000 colonies in ~ 7 hours); finally, promising colonies were picked manually [39]. This approach also has the potential to screen other types of indicators that can be expressed in bacteria, such as calcium indicators.

Many PODs require expression in mammalian cells to fold and traffic to the desired subcellular location. For instance, we have been unsuccessful at expressing genetically encoded voltage indicators based on 4-pass voltage-sensing domains [40,41] in bacteria and yeast (*unpublished results*). Even if a POD can be expressed in bacteria or yeast, improvements from screening in these organisms may not translate to higher performance in mammalian cells. For example, the brightness of FPs in bacteria is not always predictive of their brightness in mammalian cells [42]. Therefore, screening PODs in mammalian cells can be beneficial or required. However, while mammalian cells can form colonies (on plates with tissue-culture media rather than agar), visible colonies of more than 50 cells require growth for 1-2 weeks [43] rather than one day for bacteria. To pick mammalian colonies without cross-contamination, mammalian cells are typically seeded to achieve fewer than 50 colonies per plate, one order of magnitude lower than bacterial colonies [44,45]. These limitations may explain why, to our knowledge, there are no examples of high-throughput POD screening experiments using mammalian colonies.

Colony-based screening is also unsuitable for indicators reporting cellular activity via changes in subcellular localization. For example, indicators that report kinase activity by changing their relative abundance between the nucleus and cytoplasm [46] would not show net changes in colony fluorescence. Nevertheless, a growing number of studies demonstrate that manual and automated screening of colonies on agar plates remains a valuable strategy for engineering many types of PODs.

***Automating multiwell plate screening***

Given the limitations of colony-based screening, a common alternative approach is to use microscopes and plate readers to screen POD libraries with variants arrayed in 96- or 384-well plates (**Fig. 2C**). A key benefit of screening PODs using multiwell plates over agar plates is that mammalian cells can be used to express and screen PODs. Another advantage is that multiwell plates with optically clear bottoms enable high-resolution screening, with single-cell resolution if needed, using inverted microscopes. Moreover, the stage, illumination system, filter wheel, and camera/detector of microscopes and plate readers can be motorized, enabling automated data acquisition without human intervention. While motorized microscopes and plate readers can be expensive, they can be found in many academic laboratories and institutional shared facilities.

A critical downside of traditional multiwell-based screening is its limited throughput, given that variants arrayed into multiwell plates are assayed sequentially. To address this limitation, Chan *et al*. developed a fluorescence imaging system that can simultaneously image all wells of a 96-well plate in 10 s and with < 1 µm resolution [47]. However, this method requires a specialized optical system linked to a computer with significant graphic processing capabilities. Other limitations of multiwell screens are the cost, repetitive nature, and organizational challenges with preparing and screening libraries. The impact of these limitations can be mitigated by designing libraries using statistical approaches to maximize success and minimize cost [48,49]. Integrated imaging solutions — including liquid handlers, plate hotels, and incubators — can automate the preparation and screening of large numbers of plates; however, the high cost of these instruments has limited their broader adoption in academic laboratories. Given the challenges of screening multiwell plates, it is usually difficult for a single academic researcher to screen more than several 96-well plates of transfected mammalian cells daily. Fewer than $10^3$ variants can thus be screened per day, far less than the $10^4$-$10^5$ variants that can be routinely evaluated by bacterial or yeast colony screening. Nevertheless, since significant performance improvements have often been achieved by evaluating less than 1,000 POD variants, multiwell screening is a common approach for optimizing optical indicators and actuators [40,41,50].

***Automated pooled library screening by flow cytometry***

Screening pooled libraries, in which each cell expresses a different variant, can increase screening throughput over screening using multiwell plates. A common technique to screen pooled libraries, called flow cytometry, is to rapidly move cells through a capillary and evaluate their fluorescence as they cross one or more laser beams (**Fig. 2D**). In Fluorescence-Activated Cell Sorting (FACS), cells are steered toward collection or discard tubes based on user-determined fluorescence thresholds ("gates") [51,52]. A primary advantage of FACS is high throughput: modern instruments can screen up to $10^4$ cells per second. FACS has been used for POD engineering, for example, to identify brighter fluorescent proteins [53–55].

Exciting recent advances in flow cytometry open new opportunities to optimize PODs using FACS. Spectral FACS enables the measurement of fluorescence spectra, which could enable screening for different POD color variants (i.e., shifting the emission and excitation spectra). Spectral FACS can also have higher sensitivity for dim fluorescence signals [56,57]. Imaging FACS can capture (or reconstruct) images of cells flowing through the microcapillaries and obtain spatial information of individual cells [58,59]. Imaging FACS may be utilized for high-throughput POD optimization of selected spatial properties such as the subcellular localization of fluorescent-labeled proteins. For example, this technique enabled detailed cell cycle analyses that distinguish between mitotic stages [58]. However, spatial resolution remains poor compared with even traditional widefield fluorescence microscopy, limiting the ability to screen for more subtle spatial phenotypes.

Arguably the most critical drawback of FACS instruments is their inability to measure fluorescence at many time points. The lack of temporal resolution precludes longitudinal analyses of cellular dynamics and the screening for critical POD temporal properties, including photostability, response kinetics, and the peak amplitude of transient responses [38,60]. To mitigate this problem, custom microfluidic chips were designed to measure fluorescence before and after cells are presented with an analyte[61] or submitted to a photobleaching laser pulse [62,63]. The sorting speed of these devices is lower than that of conventional FACS systems by orders of magnitude. Nevertheless, these chips can still sort thousands of cells per hour; screening throughput can thus remain higher than with multiwell plate

screening. However, flow cytometry is not well adapted to measuring characteristics that require many measurements over time. Moreover, because cells are evaluated sequentially, screening PODs with slow response kinetics (e.g., several seconds or longer) may be impractically long using microfluidic flow cytometry. Finally, false positive and negative rates can also be higher than those in multiwell plate screening since the performance metrics are evaluated in single cells. Nevertheless, flow cytometry remains a popular and valuable approach for screening PODs [63–65].

***Automated microscope-based pooled library screening***

Microscope-based pooled screening approaches have been developed to combine the higher throughput of pooled screens with the ability to optimize PODs' spatial and dynamical properties (**Fig. 2E**). In typical screens, up to hundreds of thousands of cells expressing different variants are mixed, and fields-of-view containing large numbers of cells are imaged sequentially. The characteristics of individual cells are analyzed, and the cells with desirable properties are retrieved for further characterization, genotyping, or both.

A key challenge of microscope-based screens is how to automate the retrieval of the target cells. One strategy is to use automated micropipetting to aspirate the best-performing cells. This method was used to develop brighter voltage indicators after screening 12,500 individual cells [66]. Aspiration-based cell retrieval methods, while valuable, are limited in throughput because of the time required to move the micromanipulator, aspirate, eject the cell, and clean the pipette. They have been established for mammalian cells but not smaller cells like yeast and bacteria, which are commonly used for protein engineering. An alternative method, μSCALE, is to screen bacterial or yeast pooled libraries loaded into a dense array of millions of small (10-20 μm) microcapillaries [67]. The cell suspension is pipetted onto the array at a concentration that results in most microcapillaries being empty or occupied by a single cell. Incubating the array can be performed to achieve clonal expansion in each microcapillary, thereby increasing the fluorescence signal. After automated library imaging, pulsed ultraviolet light is used to excite magnetic beads mixed with the cell suspension. This process disrupts the surface tension at the bottom of the microcapillary, possibly due to bead heating and the formation of a cavitation bubble. The contents of the microcapillary are thereby released into an extraction plate located below the array. μSCALE was used for various protein engineering applications, including screening bacterial libraries to color-shift an FP from red to orange. However, further studies are needed to determine whether the μSCALE cellular release method can be used with mammalian cells, which are more fragile than yeast and bacteria.

Because μSCALE and aspiration-based screening methods are only compatible with some cell types, our group developed SPOTlight, a versatile method for screening bacteria, yeast, and mammalian cells [68]. With SPOTlight, individual cells expressing POD variants are screened, and cells expressing improved variants are optically tagged on the microscope. The optically tagged cells are subsequently recovered using FACS. Optical tagging was performed by labeling cells with a photoactivatable FP or dye that irreversibly converts from a dark state to a fluorescent state, followed by single-cell illumination using a light patterning device. Notably, the identification and optical tagging of target cells were automated. Three million single-cell variants expressed in yeast were screened using SPOTlight, leading to the identification of a bright and photostable yellow fluorescent protein (YFP) variant called mGold that is 4-5-fold more photostable than its predecessor [68]. A pre-print also recently reported using a similar approach to screen ~120,000 single cells for voltage indicators with increased brightness and response amplitude, in this case using a green-to-red photoconvertible FP for optical tagging [69].

A key benefit of microscopy-based pooled screening compared with multiwell-based screening is the much higher achievable throughput. For example, multiwell-based screening of 3 million variants – the number of YFPs variants we screened to develop mGold – would require screening four 96-well plates per day for 21 years (assuming one variant per well and screening four plates per day). By comparison, microscopy-based pooled screened enabled us to evaluate 3 million variants in eight rounds of screening, each requiring one day. Another benefit of pooled libraries is the lower cost of consumables. Screening 3 million variants would otherwise require ~30 thousand 96-well plates made from individually picked bacterial/yeast colonies or mammalian cell transfections of miniprepped DNA. In contrast, only eight wells of a 24-well plate were used for SPOTlight screening of mGold: each round of screening was conducted in one well of a 24-well plate, and a total of eight rounds of screening were conducted.

Each pooled library was produced by a single transformation reaction with yeast cells. Although microscopy-based pooled screening requires additional hardware add-ons (e.g., a digital micromirror device for SPOTlight), the cost of the add-on can be rapidly compensated by faster throughput and lower operating costs. For example, the $10^5$ variants we routinely screen in a single round of SPOTlight would cost over $100,000 with standard multiwell plate screens (given that DNA minipreps alone typically cost $1-10 per variant), compared with $30-60,000 for a digital mirror device used to selectively photoactivate cells.

There are several challenges with microscope-based pooled screening. First, as with flow cytometry pooled screens, high cell-to-cell variability in the measured properties can produce high false positive and negative rates. Retesting promising variants in a larger number of cells is thus often required to confirm the improved POD properties. Second, while cost-effective for large screens, microscope-based pooled screening techniques require expensive hardware to retrieve target cells, for example, a robotic cell picker or optical patterning device. These additional pieces of equipment must also be carefully calibrated for optimal results. Finally, sophisticated software is also needed to distinguish (segment) and characterize individual cells — although recent advances in machine learning can facilitate these tasks [70–72].

***Emerging approaches in automated POD engineering***

While screening strategies described so far used cells to express PODs, emerging high-throughput screening approaches use cell-free transcription and translation systems. As with cell-based screening, DNA libraries must first be constructed. However, rather than being transformed or transfected in cells, the libraries are expressed in a reconstituted environment containing gene expression machinery [73,74]. For example, a recent study reported a cell-free system for screening fluorescent indicators in semipermeable beads [75]. This system was deployed to engineer a lactate indicator with higher response amplitude and lower pH sensitivity than previous sensors. When bound on a coverslip, the beads could withstand buffer changes in a perfusion chamber, thereby allowing the rapid determination of indicators' responses to different lactate and pH levels.

Cell-free approaches are advantageous as they are not subject to cell-to-cell variability in POD expression or function during screening. They also obviate the need to grow and maintain cells. However, proteins optimized in cell-free environments may not fold and perform identically in cells. Variations in protein performance between cell and cell-free environments are likely prevalent for membrane proteins [76], which is a significant limitation given the importance of membrane proteins in the toolbox of optical indicators and actuators [9,60]. Nevertheless, we anticipate that cell-free approaches will be increasingly used for POD engineering in the next several years.

Because the number of ways a POD could be mutated exceeds the number of atoms in the universe [77], even pooled library methods can only sample a small fraction of the enormous sequence space. The ability to prioritize specific mutations —or at least residues to target by saturation mutagenesis— can accelerate POD engineering and increase success. Structure-guided directed evolution is a popular approach to prioritizing specific residues or mutations when the POD — or one or more of its component domains — is understood mechanistically [78]. Structured-guided approaches can benefit from computational methods that predict how mutations will affect POD function. For example, the Rosetta molecular modeling program [79] was used to design a library of light-inducible dimers. These photodimerizers were predicted to have stronger binding affinity in the dark, thereby producing larger light-driven changes in binding affinity. The computationally designed library was screened experimentally, and several variants were identified with larger binding affinity changes upon light stimulation [78].

Machine Learning (ML) is an emerging and complementary approach to guide directed evolution: POD characterization data acquired during screening is used to train a computational model to predict sequences with improved performance [80]. ML model training data can consist of individual protein sequences and their corresponding performance metrics. Pooled sequences from groups of variants (e.g., functional vs. non-functional variants or indicators with slow vs. fast kinetics) can also be used to train ML models. More sophisticated models can include information about protein structure and amino acid properties to explore novel mutations not present in the training dataset, leading to new combinations of mutations that would not be considered otherwise. While predictive models can be achieved with a low amount of data (e.g., 100-200 sequences and their corresponding

properties) [81,82], the accuracy of ML models can improve with increasing amounts of high-quality data. ML can thus benefit from automated screening.

Proof-of-concept studies used ML to increase FP fluorescence [82] and improve a fluorescent serotonin sensor[83]. ML was also used to create opsins with efficient plasma membrane localization, high conductance, and a range of deactivation kinetics [81]. These ML-designed opsins outperformed commonly used variants under some illumination conditions, enabling light-induced activation of neurons deeper in the mouse brain.

***Concluding remarks***

Nobody aspires to conduct tedious and repetitive tasks. Incorporating automation into POD engineering frees human hands, eyes, and brain to improve library design, high-throughput characterization assays, and hit selection strategies. Automation can also increase screening throughput and accuracy. The ultimate dream of POD engineers is an automated platform that can rapidly conduct all screening steps — developing libraries, evaluating variants, and selecting hits — without user involvement. This lofty goal may not be farfetched given innovations in self-learning robotic platforms [84] and automated continuous evolution systems [85,86].

***Corresponding Author***

François St-Pierre

Department of Neuroscience, and Department of Biochemistry and Molecular Biology, Baylor College of Medicine, Houston, TX, 77030, USA; Systems, Synthetic, and Physical Biology Program, and Department of Electrical and Computer Engineering, Rice University, Houston, TX 77005, USA.

https://orcid.org/0000-0001-8618-4135

Email: stpierre@bcm.edu

***Funding***

This work was supported by the McNair Medical Foundation; the John S. Dunn Foundation; Welch Foundation grants Q-2016-20190330 and Q-2016-20220331; the Klingenstein-Simons Fellowship Award in Neuroscience; NIH grants R01EB027145, U01NS113294, U01NS118288, R01EB032854; and NSF grants 1707359 and 1935265.

***Notes***

F.S.-P. holds a US patent for a genetically encoded voltage indicator (patent number US9606100 B2). F.S.-P., J.L., and Z.L., have filed a patent based on the SPOTlight pooled screening method.

**For Table of Contents use only**

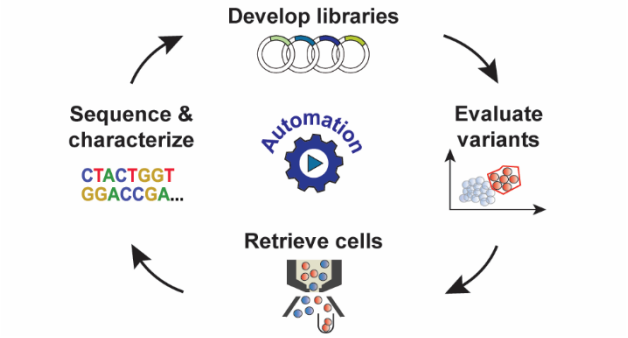

**Bibliography**

(1) Rodriguez, E. A., Campbell, R. E., Lin, J. Y., Lin, M. Z., Miyawaki, A., Palmer, A. E., Shu, X., Zhang, J., and Tsien, R. Y. (2017) The growing and glowing toolbox of fluorescent and photoactive proteins. *Trends Biochem. Sci. 42*, 111–129.

(2) Michalet, X., Pinaud, F. F., Bentolila, L. A., Tsay, J. M., Doose, S., Li, J. J., Sundaresan, G., Wu, A. M., Gambhir, S. S., and Weiss, S. (2005) Quantum dots for live cells, in vivo imaging, and diagnostics. *Science 307*, 538–544.

(3) Miller, E. W. (2016) Small molecule fluorescent voltage indicators for studying membrane potential. *Curr. Opin. Chem. Biol. 33*, 74–80.

(4) Naresh, V., and Lee, N. (2021) A Review on Biosensors and Recent Development of Nanostructured Materials-Enabled Biosensors. *Sensors 21, 1109*.

(5) Su, Y., and Hammond, M. C. (2020) RNA-based fluorescent biosensors for live cell imaging of small molecules and RNAs. *Curr. Opin. Biotechnol. 63*, 157–166.

(6) Deo, C., Abdelfattah, A. S., Bhargava, H. K., Berro, A. J., Falco, N., Farrants, H., Moeyaert, B., Chupanova, M., Lavis, L. D., and Schreiter, E. R. (2021) The HaloTag as a general scaffold for far-red tunable chemigenetic indicators. *Nat. Chem. Biol. 17*, 718–723.

(7) Leopold, A. V., Shcherbakova, D. M., and Verkhusha, V. V. (2019) Fluorescent biosensors for neurotransmission and neuromodulation: engineering and applications. *Front. Cell. Neurosci. 13*, 474.

(8) Rost, B. R., Schneider-Warme, F., Schmitz, D., and Hegemann, P. (2017) Optogenetic tools for subcellular applications in neuroscience. *Neuron 96*, 572–603.

(9) Lin, M. Z., and Schnitzer, M. J. (2016) Genetically encoded indicators of neuronal activity. *Nat. Neurosci. 19*, 1142–1153.

(10) Kostyuk, A. I., Demidovich, A. D., Kotova, D. A., Belousov, V. V., and Bilan, D. S. (2019) Circularly Permuted Fluorescent Protein-Based Indicators: History, Principles, and Classification. *Int. J. Mol. Sci. 20.*, 4200

(11) Ibraheem, A., and Campbell, R. E. (2010) Designs and applications of fluorescent protein-based biosensors. *Curr. Opin. Chem. Biol. 14*, 30–36.

(12) Greenwald, E. C., Mehta, S., and Zhang, J. (2018) Genetically encoded fluorescent biosensors illuminate the spatiotemporal regulation of signaling networks. *Chem. Rev. 118*, 11707–11794.

(13) Specht, E. A., Braselmann, E., and Palmer, A. E. (2017) A Critical and Comparative Review of Fluorescent Tools for Live-Cell Imaging. *Annu. Rev. Physiol. 79*, 93–117.

(14) Govorunova, E. G., Sineshchekov, O. A., Li, H., and Spudich, J. L. (2017) Microbial rhodopsins: diversity, mechanisms, and optogenetic applications. *Annu. Rev. Biochem. 86*, 845–872.

(15) Zhou, X. X., Pan, M., and Lin, M. Z. (2015) Investigating neuronal function with optically controllable proteins. *Front. Mol. Neurosci. 8*, 37.

(16) Ma, G., Wen, S., He, L., Huang, Y., Wang, Y., and Zhou, Y. (2017) Optogenetic toolkit for precise control of calcium signaling. *Cell Calcium 64*, 36–46.

(17) Tan, P., He, L., Huang, Y., and Zhou, Y. (2022) Optophysiology: Illuminating cell physiology with optogenetics. *Physiol. Rev. 102*, 1263–1325.

(18) Leman, J. K., Weitzner, B. D., Lewis, S. M., Adolf-Bryfogle, J., Alam, N., Alford, R. F., Aprahamian, M., Baker, D., Barlow, K. A., Barth, P., Basanta, B., Bender, B. J., Blacklock, K., Bonet, J., Boyken, S. E., Bradley, P., Bystroff, C., Conway, P., Cooper, S., Correia, B. E., and Bonneau, R. (2020) Macromolecular modeling and design in Rosetta: recent methods and frameworks. *Nat. Methods 17*, 665–680.

(19) Packer, M. S., and Liu, D. R. (2015) Methods for the directed evolution of proteins. *Nat. Rev. Genet. 16*, 379–394.

(20) Romero, P. A., and Arnold, F. H. (2009) Exploring protein fitness landscapes by directed evolution. *Nat. Rev. Mol. Cell Biol. 10*, 866–876.

(21) Yuan, L., Kurek, I., English, J., and Keenan, R. (2005) Laboratory-directed protein evolution. *Microbiol. Mol. Biol. Rev. 69*, 373–392.

(22) Hendel, S. J., and Shoulders, M. D. (2021) Directed evolution in mammalian cells. *Nat. Methods 18*, 346–357.

(23) Ai, H.-W., Baird, M. A., Shen, Y., Davidson, M. W., and Campbell, R. E. (2014) Engineering and characterizing monomeric fluorescent proteins for live-cell imaging applications. *Nat. Protoc. 9*, 910–928.

(24) Lam, A. J., St-Pierre, F., Gong, Y., Marshall, J. D., Cranfill, P. J., Baird, M. A., McKeown, M. R., Wiedenmann, J., Davidson, M. W., Schnitzer, M. J., Tsien, R. Y., and Lin, M. Z. (2012) Improving FRET dynamic range with bright green and red fluorescent proteins. *Nat. Methods 9*, 1005–1012.

(25) Crameri, A., Whitehorn, E. A., Tate, E., and Stemmer, W. P. (1996) Improved green fluorescent protein by molecular evolution using DNA shuffling. *Nat. Biotechnol. 14*, 315–319.

(26) Boyden, E. S., Zhang, F., Bamberg, E., Nagel, G., and Deisseroth, K. (2005) Millisecond-timescale, genetically targeted optical control of neural activity. *Nat. Neurosci. 8*, 1263–1268.

(27) Klapoetke, N. C., Murata, Y., Kim, S. S., Pulver, S. R., Birdsey-Benson, A., Cho, Y. K., Morimoto, T. K., Chuong, A. S., Carpenter, E. J., Tian, Z., Wang, J., Xie, Y., Yan, Z., Zhang, Y., Chow, B. Y., Surek, B., Melkonian, M., Jayaraman, V., Constantine-Paton, M., Wong, G. K.-S., and Boyden, E. S. (2014) Independent optical excitation of distinct neural populations. *Nat. Methods 11*, 338–346.

(28) Govorunova, E. G., Gou, Y., Sineshchekov, O. A., Li, H., Lu, X., Wang, Y., Brown, L. S., St-Pierre, F., Xue, M., and Spudich, J. L. (2022) Kalium channelrhodopsins are natural light-gated potassium channels that mediate optogenetic inhibition. *Nat. Neurosci. 25*, 967–974.

(29) Campbell, B. C., Nabel, E. M., Murdock, M. H., Lao-Peregrin, C., Tsoulfas, P., Blackmore, M. G., Lee, F. S., Liston, C., Morishita, H., and Petsko, G. A. (2020) mGreenLantern: a bright monomeric fluorescent protein with rapid expression and cell filling properties for neuronal imaging. *Proc Natl Acad Sci USA 117*, 30710–30721.

(30) Marshel, J. H., Kim, Y. S., Machado, T. A., Quirin, S., Benson, B., Kadmon, J., Raja, C., Chibukhchyan, A., Ramakrishnan, C., Inoue, M., Shane, J. C., McKnight, D. J., Yoshizawa, S., Kato, H. E., Ganguli, S., and Deisseroth, K. (2019) Cortical layer-specific critical dynamics triggering perception. *Science 365, aaw5202*.

(31) Qian, Y., Piatkevich, K. D., Mc Larney, B., Abdelfattah, A. S., Mehta, S., Murdock, M. H., Gottschalk, S., Molina, R. S., Zhang, W., Chen, Y., Wu, J., Drobizhev, M., Hughes, T. E., Zhang, J., Schreiter, E. R., Shoham, S., Razansky, D., Boyden, E. S., and Campbell, R. E. (2019) A genetically encoded near-infrared fluorescent calcium ion indicator. *Nat. Methods 16*, 171–174.

(32) Aggarwal, A., Liu, R., Chen, Y., Ralowicz, A. J., Bergerson, S. J., Tomaska, F., Hanson, T. L., Hasseman, J. P., Reep, D., Tsegaye, G., Yao, P., Ji, X., Kloos, M., Walpita, D., Patel, R., Tilberg, P. W., Mohar, B., The GENIE Project Team, Looger, L. L., Marvin, J. S., and Podgorski, K. (2022) Glutamate indicators with improved activation kinetics and localization for imaging synaptic transmission. *BioRxiv*.

(33) Fabritius, A., Ng, D., Kist, A. M., Erdogan, M., Portugues, R., and Griesbeck, O. (2018) Imaging-Based Screening Platform Assists Protein Engineering. *Cell Chem. Biol. 25*, 1554-1561.e8.

(34) Svoboda, K., and Yasuda, R. (2006) Principles of two-photon excitation microscopy and its applications to neuroscience. *Neuron 50*, 823–839.

(35) Helmchen, F., and Denk, W. (2005) Deep tissue two-photon microscopy. *Nat. Methods 2*, 932–940.

(36) Drobizhev, M., Makarov, N. S., Tillo, S. E., Hughes, T. E., and Rebane, A. (2011) Two-photon absorption properties of fluorescent proteins. *Nat. Methods 8*, 393–399.

(37) Adhikari, D. P., Biener, G., Stoneman, M. R., Badu, D. N., Paprocki, J. D., Eis, A., Park, P. S.-H., Popa, I., and Raicu, V. (2021) Comparative photophysical properties of some widely used fluorescent proteins under two-photon excitation conditions. *Spectrochim. Acta A Mol. Biomol. Spectrosc. 262*, 120133.

(38) Liu, Z., Lu, X., Villette, V., Gou, Y., Colbert, K. L., Lai, S., Guan, S., Land, M. A., Lee, J., Assefa, T., Zollinger, D. R., Korympidou, M. M., Vlasits, A. L., Pang, M. M., Su, S., Cai, C., Froudarakis, E., Zhou, N., Patel, S. S., Smith, C. L., and St-Pierre, F. (2022) Sustained deep-tissue voltage recording using a fast indicator evolved for two-photon microscopy. *Cell 185, 3408-3425.e29*.

(39) Molina, R. S., King, J., Franklin, J., Clack, N., McRaven, C., Goncharov, V., Flickinger, D., Svoboda, K., Drobizhev, M., and Hughes, T. E. (2020) High throughput instrument to screen fluorescent proteins under two-photon excitation. *Biomed. Opt. Express 11*, 7192–7203.

(40) Wan, J., Peng, W., Li, X., Qian, T., Song, K., Zeng, J., Deng, F., Hao, S., Feng, J., Zhang, P., Zhang, Y., Zou, J., Pan, S., Shin, M., Venton, B. J., Zhu, J. J., Jing, M., Xu, M., and Li, Y. (2021) A genetically encoded sensor for measuring serotonin dynamics. *Nat. Neurosci. 24*, 746–752.

(41) Duffet, L., Kosar, S., Panniello, M., Viberti, B., Bracey, E., Zych, A. D., Radoux-Mergault, A., Zhou, X., Dernic, J., Ravotto, L., Tsai, Y.-C., Figueiredo, M., Tyagarajan, S. K., Weber, B., Stoeber, M., Gogolla, N., Schmidt, M. H., Adamantidis, A. R., Fellin, T., Burdakov, D., and Patriarchi, T. (2022) A genetically encoded sensor for in vivo imaging of orexin neuropeptides. *Nat. Methods 19*, 231–241.

(42) Balleza, E., Kim, J. M., and Cluzel, P. (2018) Systematic characterization of maturation time of fluorescent proteins in living cells. *Nat. Methods 15*, 47–51.

(43) Crowley, L. C., Christensen, M. E., and Waterhouse, N. J. (2016) Measuring Survival of Adherent Cells with the Colony-Forming Assay. *Cold Spring Harb. Protoc. 2016, 721*.

(44) Mathupala, S., and Sloan, A. A. (2009) An agarose-based cloning-ring anchoring method for isolation of viable cell clones. *BioTechniques 46*, 305–307.

(45) Natarajan, S., Chow, T. T., Shay, J. W., and Wright, W. E. (2007) Replica plating of mammalian cells using low melt agarose. *Cytotechnology 54*, 145–147.

(46) Regot, S., Hughey, J. J., Bajar, B. T., Carrasco, S., and Covert, M. W. (2014) High-sensitivity measurements of multiple kinase activities in live single cells. *Cell 157*, 1724–1734.

(47) Chan, A. C. S., Kim, J., Pan, A., Xu, H., Nojima, D., Hale, C., Wang, S., and Yang, C. (2019) Parallel Fourier ptychographic microscopy for high-throughput screening with 96 cameras (96 Eyes). *Sci. Rep. 9*, 11114.

(48) Acevedo-Rocha, C. G., Reetz, M. T., and Nov, Y. (2015) Economical analysis of saturation mutagenesis experiments. *Sci. Rep. 5*, 10654.

(49) Nov, Y. (2012) When second best is good enough: another probabilistic look at saturation mutagenesis. *Appl. Environ. Microbiol. 78*, 258–262.

(50) Chen, T.-W., Wardill, T. J., Sun, Y., Pulver, S. R., Renninger, S. L., Baohan, A., Schreiter, E. R., Kerr, R. A., Orger, M. B., Jayaraman, V., Looger, L. L., Svoboda, K., and Kim, D. S. (2013) Ultrasensitive fluorescent proteins for imaging neuronal activity. *Nature 499*, 295–300.

(51) Adan, A., Alizada, G., Kiraz, Y., Baran, Y., and Nalbant, A. (2017) Flow cytometry: basic principles and applications. *Crit. Rev. Biotechnol. 37*, 163–176.

(52) McKinnon, K. M. (2018) Flow cytometry: an overview. *Curr. Protoc. Immunol. 120*, 5.1.1-5.1.11.

(53) Wang, L., Jackson, W. C., Steinbach, P. A., and Tsien, R. Y. (2004) Evolution of new nonantibody proteins via iterative somatic hypermutation. *Proc Natl Acad Sci USA 101*, 16745–16749.

(54) Wang, L., and Tsien, R. Y. (2006) Evolving proteins in mammalian cells using somatic hypermutation. *Nat. Protoc. 1*, 1346–1350.

(55) Cormack, B. P., Valdivia, R. H., and Falkow, S. (1996) FACS-optimized mutants of the green fluorescent protein (GFP). *Gene 173*, 33–38.

(56) Niewold, P., Ashhurst, T. M., Smith, A. L., and King, N. J. C. (2020) Evaluating spectral cytometry for immune profiling in viral disease. *Cytometry A 97*, 1165–1179.

(57) Nolan, J. P. (2022) The evolution of spectral flow cytometry. *Cytometry 101, 812-817*.

(58) Schraivogel, D., Kuhn, T. M., Rauscher, B., Rodríguez-Martínez, M., Paulsen, M., Owsley, K., Middlebrook, A., Tischer, C., Ramasz, B., Ordoñez-Rueda, D., Dees, M., Cuylen-Haering, S., Diebold, E., and Steinmetz, L. M. (2022) High-speed fluorescence image-enabled cell sorting. *Science 375*, 315–320.

(59) Nitta, N., Sugimura, T., Isozaki, A., Mikami, H., Hiraki, K., Sakuma, S., Iino, T., Arai, F., Endo, T., Fujiwaki, Y., Fukuzawa, H., Hase, M., Hayakawa, T., Hiramatsu, K., Hoshino, Y., Inaba, M., Ito, T., Karakawa, H., Kasai, Y., Koizumi, K., and Goda, K. (2018) Intelligent Image-Activated Cell Sorting. *Cell 175*, 266-276.e13.

(60) Yang, H. H., and St-Pierre, F. (2016) Genetically encoded voltage indicators: opportunities and challenges. *J. Neurosci. 36*, 9977–9989.

(61) Fiedler, B. L., Van Buskirk, S., Carter, K. P., Qin, Y., Carpenter, M. C., Palmer, A. E., and Jimenez, R. (2017) Droplet Microfluidic Flow Cytometer For Sorting On Transient Cellular Responses Of Genetically-Encoded Sensors. *Anal. Chem. 89*, 711–719.

(62) Lubbeck, J. L., Dean, K. M., Ma, H., Palmer, A. E., and Jimenez, R. (2012) Microfluidic flow cytometer for quantifying photobleaching of fluorescent proteins in cells. *Anal. Chem. 84*, 3929–3937.

(63) Dean, K. M., Lubbeck, J. L., Davis, L. M., Regmi, C. K., Chapagain, P. P., Gerstman, B. S., Jimenez, R., and Palmer, A. E. (2015) Microfluidics-based selection of red-fluorescent proteins with decreased rates of photobleaching. *Integr Biol (Camb) 7*, 263–273.

(64) Mukherjee, S., Hung, S.-T., Douglas, N., Manna, P., Thomas, C., Ekrem, A., Palmer, A. E., and Jimenez, R. (2020) Engineering of a Brighter Variant of the FusionRed Fluorescent Protein Using Lifetime Flow Cytometry and Structure-Guided Mutations. *Biochemistry 59*, 3669–3682.

(65) Manna, P., Hung, S.-T., Mukherjee, S., Friis, P., Simpson, D. M., Lo, M. N., Palmer, A. E., and Jimenez, R. (2018) Directed evolution of excited state lifetime and brightness in FusionRed using a microfluidic sorter. *Integr Biol (Camb) 10*, 516–526.

(66) Piatkevich, K. D., Jung, E. E., Straub, C., Linghu, C., Park, D., Suk, H.-J., Hochbaum, D. R., Goodwin, D., Pnevmatikakis, E., Pak, N., Kawashima, T., Yang, C.-T., Rhoades, J. L., Shemesh, O., Asano, S., Yoon, Y.-G., Freifeld, L., Saulnier, J. L., Riegler, C., Engert, F., and Boyden, E. S. (2018) A robotic multidimensional directed evolution approach applied to fluorescent voltage reporters. *Nat. Chem. Biol. 14*, 352–360.

(67) Chen, B., Lim, S., Kannan, A., Alford, S. C., Sunden, F., Herschlag, D., Dimov, I. K., Baer, T. M., and Cochran, J. R. (2016) High-throughput analysis and protein engineering using microcapillary arrays. *Nat. Chem. Biol. 12*, 76–81.

(68) Lee, J., Liu, Z., Suzuki, P. H., Ahrens, J. F., Lai, S., Lu, X., Guan, S., and St-Pierre, F. (2020) Versatile phenotype-activated cell sorting. *Sci. Adv. 6, eabb7438*.

(69) Tian, H., Davis, H. C., Wong-Campos, J. D., Fan, L. Z., Gmeiner, B., Begum, S., Werley, C. A., Borja, G. B., Upadhyay, H., Shah, H., Jacques, J., Park, P., Qi, Y., Parot, V., Deisseroth, K., and Cohen, A. E. (2021) All-optical electrophysiology with improved genetically encoded voltage indicators reveals interneuron network dynamics in vivo. *BioRxiv*.

(70) Moen, E., Bannon, D., Kudo, T., Graf, W., Covert, M., and Van Valen, D. (2019) Deep learning for cellular image analysis. *Nat. Methods 16*, 1233–1246.

(71) Stringer, C., Wang, T., Michaelos, M., and Pachitariu, M. (2021) Cellpose: a generalist algorithm for cellular segmentation. *Nat. Methods 18*, 100–106.

(72) Berg, S., Kutra, D., Kroeger, T., Straehle, C. N., Kausler, B. X., Haubold, C., Schiegg, M., Ales, J., Beier, T., Rudy, M., Eren, K., Cervantes, J. I., Xu, B., Beuttenmueller, F., Wolny, A., Zhang, C., Koethe, U., Hamprecht, F. A., and Kreshuk, A. (2019) ilastik: interactive machine learning for (bio)image analysis. *Nat. Methods 16*, 1226–1232.

(73) Contreras-Llano, L. E., and Tan, C. (2018) High-throughput screening of biomolecules using cell-free gene expression systems. *Synth. Biol. 3, eysy012*.

(74) Zhang, Y., Minagawa, Y., Kizoe, H., Miyazaki, K., Iino, R., Ueno, H., Tabata, K. V., Shimane, Y., and Noji, H. (2019) Accurate high-throughput screening based on digital protein synthesis in a massively parallel femtoliter droplet array. *Sci. Adv. 5*, eaav8185.

(75) Koveal, D., Rosen, P. C., Meyer, D. J., Díaz-García, C. M., Wang, Y., Cai, L.-H., Chou, P. J., Weitz, D. A., and Yellen, G. (2022) A high-throughput multiparameter screen for accelerated development and optimization of soluble genetically encoded fluorescent biosensors. *Nat. Commun. 13*, 2919.

(76) Roos, C., Kai, L., Proverbio, D., Ghoshdastider, U., Filipek, S., Dötsch, V., and Bernhard, F. (2013) Co-translational association of cell-free expressed membrane proteins with supplied lipid bilayers. *Mol. Membr. Biol. 30*, 75–89.

(77) Lee, J., and St-Pierre, F. (2022) A blueprint for glow tag engineering. *Nat. Rev. Chem. 6*, 7–8.

(78) Goedhart, J., von Stetten, D., Noirclerc-Savoye, M., Lelimousin, M., Joosen, L., Hink, M. A., van Weeren, L., Gadella, T. W. J., and Royant, A. (2012) Structure-guided evolution of cyan fluorescent proteins towards a quantum yield of 93%. *Nat. Commun. 3*, 751.

(79) Leaver-Fay, A., Tyka, M., Lewis, S. M., Lange, O. F., Thompson, J., Jacak, R., Kaufman, K., Renfrew, P. D., Smith, C. A., Sheffler, W., Davis, I. W., Cooper, S., Treuille, A., Mandell, D. J., Richter, F., Ban, Y.-E. A., Fleishman, S. J., Corn, J. E., Kim, D. E., Lyskov, S., and Bradley, P. (2011) ROSETTA3: an object-oriented software suite for the simulation and design of macromolecules. *Meth. Enzymol. 487*, 545–574.

(80) Yang, K. K., Wu, Z., and Arnold, F. H. (2019) Machine-learning-guided directed evolution for protein engineering. *Nat. Methods 16*, 687–694.

(81) Bedbrook, C. N., Yang, K. K., Robinson, J. E., Mackey, E. D., Gradinaru, V., and Arnold, F. H. (2019) Machine learning-guided channelrhodopsin engineering enables minimally invasive optogenetics. *Nat. Methods 16*, 1176–1184.

(82) Saito, Y., Oikawa, M., Nakazawa, H., Niide, T., Kameda, T., Tsuda, K., and Umetsu, M. (2018) Machine-Learning-Guided Mutagenesis for Directed Evolution of Fluorescent Proteins. *ACS Synth. Biol. 7*, 2014–2022.

(83) Unger, E. K., Keller, J. P., Altermatt, M., Liang, R., Matsui, A., Dong, C., Hon, O. J., Yao, Z., Sun, J., Banala, S., Flanigan, M. E., Jaffe, D. A., Hartanto, S., Carlen, J., Mizuno, G. O., Borden, P. M., Shivange, A. V., Cameron, L. P., Sinning, S., Underhill, S. M., and Tian, L. (2020) Directed evolution of a selective and sensitive serotonin sensor via machine learning. *Cell 183*, 1986-2002.e26.

(84) HamediRad, M., Chao, R., Weisberg, S., Lian, J., Sinha, S., and Zhao, H. (2019) Towards a fully automated algorithm driven platform for biosystems design. *Nat. Commun. 10*, 5150.

(85) Molina, R. S., Rix, G., Mengiste, A. A., Álvarez, B., Seo, D., Chen, H., Hurtado, J. E., Zhang, Q., García-García, J. D., Heins, Z. J., Almhjell, P. J., Arnold, F. H., Khalil, A. S., Hanson, A. D., Dueber, J. E., Schaffer, D. V., Chen, F., Kim, S., Fernández, L. Á., Shoulders, M. D., and Liu, C. C. (2022) In vivo hypermutation and continuous evolution. *Nat. Rev. Methods Primers 2*, 36.

(86) Morrison, M. S., Podracky, C. J., and Liu, D. R. (2020) The developing toolkit of continuous directed evolution. *Nat. Chem. Biol. 16*, 610–619.

(87) Babakhanova, S., Jung, E. E., Namikawa, K., Zhang, H., Wang, Y., Subach, O. M., Korzhenevskiy, D. A., Rakitina, T. V., Xiao, X., Wang, W., Shi, J., Drobizhev, M., Park, D., Eisenhard, L., Tang, H., Köster, R. W., Subach, F. V., Boyden, E. S., and Piatkevich, K. D. (2022) Rapid directed molecular evolution of fluorescent proteins in mammalian cells. *Protein Sci. 31*, 728–751.

(88) Tian, L., Hires, S. A., Mao, T., Huber, D., Chiappe, M. E., Chalasani, S. H., Petreanu, L., Akerboom, J., McKinney, S. A., Schreiter, E. R., Bargmann, C. I., Jayaraman, V., Svoboda, K., and Looger, L. L. (2009) Imaging neural activity in worms, flies and mice with improved GCaMP calcium indicators. *Nat. Methods 6*, 875–881.

(89) Cho, Y. K., Park, D., Yang, A., Chen, F., Chuong, A. S., Klapoetke, N. C., and Boyden, E. S. (2019) Multidimensional screening yields channelrhodopsin variants having improved photocurrent and order-of-magnitude reductions in calcium and proton currents. *J. Biol. Chem. 294*, 3806–3821.

(90) Guntas, G., Hallett, R. A., Zimmerman, S. P., Williams, T., Yumerefendi, H., Bear, J. E., and Kuhlman, B. (2015) Engineering an improved light-induced dimer (iLID) for controlling the localization and activity of signaling proteins. *Proc Natl Acad Sci USA 112*, 112–117.

(91) He, L., Wang, L., Zeng, H., Tan, P., Ma, G., Zheng, S., Li, Y., Sun, L., Dou, F., Siwko, S., Huang, Y., Wang, Y., and Zhou, Y. (2021) Engineering of a bona fide light-operated calcium channel. *Nat. Commun. 12*, 164.